Context-Dependent Substrate Recognition by Protein Farnesyltransferase[†]

James L. Hougland,[‡] Corissa L. Lamphear,[§] Sarah A. Scott,[||,⊥] Richard A. Gibbs,[||] and Carol A. Fierke*[,‡,§]

Departments of Chemistry and Biological Chemistry, University of Michigan, Ann Arbor, Michigan 48109, and Department of Medicinal Chemistry and Molecular Pharmacology, School of Pharmacy and Pharmaceutical Sciences, Purdue University, West Lafayette, Indiana 47907

Received September 8, 2008; Revised Manuscript Received December 12, 2008

ABSTRACT: Prenylation is a posttranslational modification whereby C-terminal lipidation leads to protein localization to membranes. A C-terminal "Ca_1a_2X" sequence has been proposed as the recognition motif for two prenylation enzymes, protein farnesyltransferase (FTase) and protein geranylgeranyltransferase type I. To define the parameters involved in recognition of the a_2 residue, we performed structure−activity analysis which indicates that FTase discriminates between peptide substrates based on both the hydrophobicity and steric volume of the side chain at the a_2 position. For nonpolar side chains, the dependence of the reactivity on side chain volume at this position forms a pyramidal pattern with a maximal activity near the steric volume of valine. This discrimination occurs at a step in the kinetic mechanism that is at or before the farnesylation step. Furthermore, a_2 selectivity is also affected by the identity of the adjacent X residue, leading to context-dependent substrate recognition. Context-dependent a_2 selectivity suggests that FTase recognizes the sequence downstream of the conserved cysteine as a set of two or three cooperative, interconnected recognition elements as opposed to three independent amino acids. These findings expand the pool of proposed FTase substrates in cells. A better understanding of the molecular recognition of substrates performed by FTase will aid in both designing new FTase inhibitors as therapeutic agents and characterizing proteins involved in prenylation-dependent cellular pathways.

Protein farnesyltransferase (FTase)[1] and protein geranylgeranyltransferase type I (GGTase-I) are members of the prenyltransferase family of sulfur alkyltransferases (reviewed in refs *1* and *2*). These enzymes, which are both heterodimers composed of α and β subunits, employ a zinc ion to catalyze the covalent attachment of a 15-carbon farnesyl group from farnesyl diphosphate (FPP) or a 20-carbon geranylgeranyl group from geranylgeranyl diphosphate (GGPP) to a cysteine residue near the C-terminus of a protein substrate (*2, 3*). The attached lipid aids in localization of proteins to cellular membranes and enhances protein−protein interactions (*4, 5*). Prenylation is required for the proper function of many proteins, including members of the Ras and Rho superfamilies of small GTPases (*1, 6*). While many proteins have been experimentally shown to be prenylated *in vivo* (*7*−*10*), the extent of prenylation within the proteome remains unclear.

Farnesyltransferase inhibitors (FTIs) are in development as therapeutics to treat cancer, parasitic infection, and other medical conditions (*11*−*13*). Defining the prenylation-dependent pathways potentially responsible for the efficacy of these treatments could provide valuable insights for development of novel pharmaceuticals. Understanding the *in vivo* substrate selectivity of FTase and GGTase-I constitutes an important step toward characterizing the prenylated proteins involved in these pathways. Based on comparison of known prenylated proteins, both FTase and GGTase-I have been proposed to recognize protein or peptide substrates containing a C-terminal "Ca_1a_2X" sequence (*14*−*20*). In this model, "C" refers to a cysteine residue three residues removed from the C-terminus that is prenylated at the thiol group to form a thioether, "a" refers to any aliphatic amino acid, and "X" refers to a subset of amino acids that are proposed to determine specificity for FTase (methionine, serine, glutamine, and alanine) or GGTase-I (leucine and phenylalanine). Expanding upon the "Ca_1a_2X" box paradigm, bioinformatic analysis and biochemical studies of known substrates and related proteins indicate that sequences immediately upstream of the conserved cysteine residue may also play a role in substrate selectivity (*8, 9, 21*).

Biochemical studies of prenyltransferase substrate specificity indicate that recognition of peptide substrates is more complex than originally proposed. For instance, although FTase and GGTase-I specificity is determined predominantly

[†] This work was funded by National Institutes of Health (NIH) Grants GM40602 to C.A.F. and CA78819 to R.A.G. and by NIH Postdoctoral Fellowship GM78894 to J.L.H. Its contents are solely the responsibility of the authors and do not necessarily represent the official views of NIGMS.

* To whom correspondence should be addressed: telephone, 734-936-2678; fax, 734-647-4865; e-mail, fierke@umich.edu.

[‡] Department of Chemistry, University of Michigan.

[§] Department of Biological Chemistry, University of Michigan.

[||] Department of Medicinal Chemistry and Molecular Pharmacology, Purdue University.

[⊥] Present address: Department of Pharmacology, Vanderbilt University, Nashville, TN 37232.

[1] Abbreviations: FTase, protein farnesyltransferase; GGTase-I, protein geranylgeranyltransferase type I; FPP, farnesyl diphosphate; GGPP, geranylgeranyl diphosphate; WT, wild type; E, enzyme; E·FPP, enzyme−farnesyl diphosphate complex; HEPES, *N*-(2-hydroxyethyl)piperazine-*N*′-2-ethanesulfonic acid; HEPPSO, *N*-(2-hydroxyethyl)piperazine-*N*′-2-hydroxypropanesulfonic acid; TCEP, tris(2-carboxyethyl)phosphine; HPLC, high-pressure liquid chromatography; TFA, trifluoroacetic acid; MDCC, *N*-[2-(1-maleimidyl)ethyl]-7-(diethylamino)coumarin-3-carboxamide; PP_iase, inorganic pyrophosphatase; dns, dansyl.

10.1021/bi801710g CCC: $40.75
Published on Web 02/06/2009

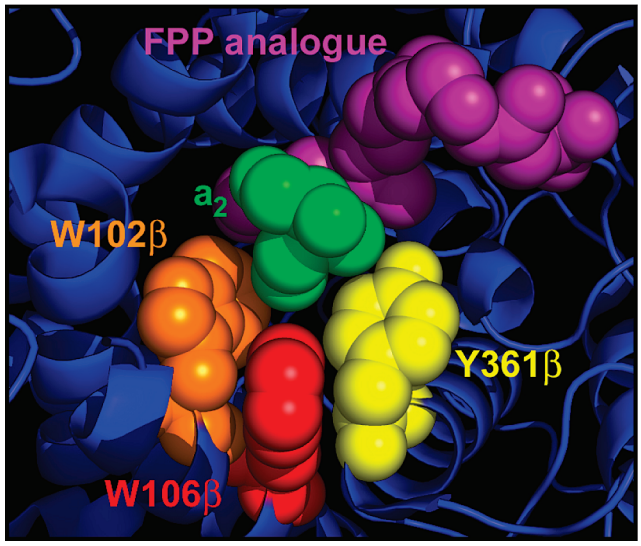

FIGURE 1: Structure of a peptide substrate bound to FTase illustrating the a_2 residue binding site. The a_2 residue of the peptide substrate KKKSKTKCVIM (green) is surrounded by residues W102β (orange), W106β (red), and Y361β (yellow) within the active site of FTase. The a_2 residue also contacts the isoprenoid tail of the FPP analogue inhibitor FPT-II (purple). Figure derived from PDB ID 1D8D and adapted from ref *10*.

by the X residue (*14, 17*−*20, 22*−*26*), some substrates react efficiently with both enzymes (*14, 26*). Peptide substrate specificity also depends on interactions of the peptide with the FPP cosubstrate, as peptide substrate reactivity can be altered in a sequence-dependent manner in the presence of FPP analogues (*27*−*29*). As these findings reflect, understanding FTase and GGTase-I substrate specificity will require identification and energetic characterization of interactions involved in substrate recognition.

As crystallographic structures of FTase and GGTase-I complexed with peptide substrates have become available, the "Ca_1a_2X" model has been modified and interpreted in the context of the active site environment. Surveys of known prenylated proteins suggest that selectivity at the a_1 position is rather relaxed, a finding consistent with structural studies which indicate that the a_1 residue of the peptide substrate is exposed to solvent within the interface of the FTase α and β subunits (*8, 10*). In contrast to the a_1 position, naturally prenylated proteins appear to favor a subset of moderately sized hydrophobic amino acids (valine, isoleucine, leucine, methionine, and threonine) at the a_2 position (*9*). The structural basis for this selectivity at the a_2 position is proposed to be due to the hydrophobic nature of the active site surrounding the a_2 residue, largely composed of two tryptophan residues (W102β and W106β), a tyrosine residue (Y361β), and the third isoprenoid unit of the FPP mimetic inhibitor present in the crystal structure (Figure 1) (*10*).

The convergence of sequence preferences from known FTase substrates and potential interactions observed within the active site structures provides valuable insight into the basis of FTase substrate selectivity. However, the functional mechanism by which substrate−enzyme interactions are transduced into differential substrate reactivity with FTase remains largely undefined. To understand how FTase recognizes various a_2 residues and then preferentially catalyzes turnover of a subset of potential substrates, the specific attributes that FTase recognizes at the a_2 position need to be identified.

In this study, we have applied structure−function analysis to define the specific selectivity criteria that FTase employs to recognize the a_2 residue of substrate peptides. We measured the reactivity of FTase with several panels of peptides wherein the a_2 residue is substituted with all 20 amino acids while keeping the remainder of the Ca_1a_2X sequence constant. Correlation of peptide reactivity within each panel against both the amino acid polarity and steric volume of the a_2 residue indicates that FTase recognizes both the size and hydrophobicity of the residue at the a_2 position, contrasting with the predominantly polarity-based recognition observed at the X residue (*21*). Furthermore, comparison across peptide panels indicates that a_2 selectivity is also affected by the identity of the adjacent X residue, leading to context-dependent substrate recognition. When X is alanine or serine, substrate selectivity is based on both polarity and steric discrimination, leading to a small number of side chains that confer efficient catalysis in this context. In contrast, in the presence of glutamine and methionine at the X position, recognition of the a_2 residue is predominantly due to polarity; substrates with a variety of amino acids at the a_2 position are readily farnesylated. These findings suggest that the current model describing FTase selectivity reflects only a subset of potential FTase substrates, raising the possibility of novel FTase substrates whose C-terminal sequences do not conform to the canonical Ca_1a_2X motif.

MATERIALS AND METHODS

Miscellaneous Methods. All assays were performed at 25 °C. All curve fitting was performed with Graphpad Prism (Graphpad Software, San Diego, CA). Farnesyl diphosphate (FPP) was purchased from Sigma. Dansylated peptides were synthesized by Sigma-Genosys (The Woodlands, TX) in the Pepscreen format. Peptide purities were ≥75%, with the majority of peptides examined exhibiting >90% purity, as determined by HPLC (Alltech Nucleosil C-18 column), with a gradient from water containing 0.1% TFA to 45% acetonitrile in water containing 0.1% TFA flowing at 1 mL/min over 25 min; peptides were detected by UV absorption at 220 nm. Major contaminants consist of smaller peptide fragments, as indicated by mass spectrometry, that are not efficient substrates for FTase (*24, 30, 31*). Peptides were solubilized in absolute ethanol containing 10% (v/v) DMSO and stored at −80 °C. Peptide concentrations were determined spectrophotometrically at 412 nm by reaction of the cysteine thiol with 5,5′-dithiobis(2-nitrobenzoic acid), using an extinction coefficient of 14150 M^{-1} cm^{-1} (*32*). Inorganic pyrophosphatase from bakers' yeast, 7-methylguanosine, and purine nucleoside phosphorylase were purchased from Sigma (St. Louis, MO).

Preparation of Wild-Type FTase. Wild-type FTase was expressed in BL21(DE3) *Escherichia coli* using a pET23aPFT vector and purified as described previously (*33, 34*). Briefly, following induction with isopropyl β-D-1-thiogalactopyranoside for 16 h at 25 °C, cells were lysed and FTase was fractionated by sequential DE53 DEAE-cellulose and POROS HQ-20 anion-exchange columns, both eluted by a NaCl gradient. FTase concentration was determined by active

Table 1: $k_{cat}/K_M^{peptide}$ Values for Farnesylation of Dansyl-GCVa$_2$X Peptides Catalyzed by FTase

			$k_{cat}/K_M^{peptide}$ (mM^{-1} s^{-1})[c]			
a_2	residue volume (Å^3)[a]	$\Delta G_{transfer}$ (kcal/mol)[b]	X = A	X = S	X = Q	X = M
K	168.6	−1.35	<0.004[e]	0.27 ± 0.02	1.9 ± 0.5	1.3 ± 0.3
D	111.1	−1.05	<0.004[e]	0.08 ± 0.02	<0.004[e]	0.004 ± 0.003
E	138.4	−0.87	<0.004[e]	0.5 ± 0.3	<0.004[e]	0.7 ± 0.4
N	114.1	−0.82	0.6 ± 0.3	3.6 ± 0.9	17 ± 7	26 ± 9
Q	143.8	−0.3	6.8 ± 0.9	45 ± 9	32 ± 7	10 ± 10
S	89	−0.05	3.2 ± 0.6	22 ± 5	33 ± 8	70 ± 20
G	60.1	0	1.6 ± 0.3	3.5 ± 0.3	9.4 ± 0.9	21 ± 3
H	153.2	0.18	1.1 ± 0.5	1.9 ± 0.3	4 ± 2	7 ± 3
T	116.1	0.35	11 ± 2	100 ± 20	50 ± 10	130 ± 50
A	88.6	0.42	3.9 ± 0.4	35 ± 2	29 ± 2	80 ± 10
P	112.7	0.98	3.4 ± 0.6	52 ± 7	12 ± 1	30 ± 10
Y	193.6	1.31	7 ± 2	2.1 ± 0.2	40 ± 10	100 ± 20
V	140	1.66	90 ± 10	320 ± 20	60 ± 30	150 ± 40
M	162.9	1.67	80 ± 30	160 ± 40	110 ± 10	270 ± 40
C	108.5	2.09	nd[d]	1.4 ± 0.4	nd[d]	nd[d]
L	166.7	2.31	70 ± 20	170 ± 40	60 ± 20	250 ± 30
F	189.9	2.43	40 ± 10	23 ± 4	130 ± 40	100 ± 20
I	166.7	2.45	120 ± 10	130 ± 30	110 ± 30	110 ± 30
W	227.8	3.06	10 ± 2	5 ± 1	50 ± 20	70 ± 10

[a] From ref *43*. [b] From ref *42*. [c] The steady-state kinetic parameters were determined at saturating FPP (10 μM) and varying peptide concentrations (0.2−10 μM peptide) in 20−100 nM FTase under conditions described in Materials and Methods. [d] Not determined due to severe substrate inhibition. [e] Upper limit for $k_{cat}/K_M^{peptide}$ based on assay sensitivity.

site titration using dansyl-GCVLS (*33*). Following dialysis into HT buffer (50 mM HEPES, pH 7.8, 2 mM TCEP), FTase was concentrated to 220 μM, aliquoted, and stored at −80 °C.

Preparation of S99βA and W102βA Mutant FTases. S99βA and W102βA mutations were introduced into the pET23aPFT plasmid using QuikChange XL methodology (Stratagene). Following confirmation of the desired mutation by sequencing, mutant FTases were expressed and purified using the same protocol as WT FTase.

Peptide Panel Design. Short peptides containing the Ca$_1$a$_2$X sequence can serve as competent substrates for FTase (*35*), simplifying access to substrate panels with exhaustive amino acid substitution at a given position. A glycine residue was appended upstream of the conserved cysteine to avoid inhibitory interactions between the peptide substrate N-terminal amino group and the FPP cosubstrate (*36*), and a dansyl fluorophore was added at the N-terminus to allow use of a previously developed fluorescence-based assay of prenylation activity (*35, 37*).

Steady-State Kinetics. Steady-state kinetics were determined for FTase from a time-dependent increase in fluorescence (λ_{ex} 340 nm, λ_{em} 520 nm) upon farnesylation of the dansylated peptide (*35, 37*). Assays were performed with 0.2−10 μM dansylated peptide, 20−100 nM FTase, 10 μM FPP, 50 mM HEPPSO, pH 7.8, 5 mM tris(2-carboxyethyl)phosphine (TCEP), 5 mM $MgCl_2$, and 10 μM $ZnCl_2$ at 25 °C in a 96-well plate (Corning). Peptides were incubated in reaction buffer for 20 min prior to initiation by addition of FTase and FPP, with the FTase concentration at least 5-fold lower than the peptide concentration. Fluorescence was measured as a function of time (intervals of 9−240 s) in a POLARstar Galaxy plate reader (BMG Labtechnologies, Durham, NC) to define both the initial linear velocity and the reaction end point. The total fluorescence change observed upon reaction completion was divided by the initial concentration of the peptide substrate in a given reaction to yield a conversion from fluorescence units to product concentration; these values were averaged over several peptide concentrations to produce an amplitude conversion (Amp_{conv}). The linear initial rate, in fluorescence intensity per second, was then converted to a velocity (μM product produced per second) using eq 1, where V is velocity in μM s^{-1}, R is the velocity of the reaction in fluorescence units per second, and Amp_{conv} refers to the ratio described above in fluorescence units per μM product.

$$V = \frac{R}{Amp_{conv}} \quad (1)$$

To confirm that farnesylation of the dansyl-GCVa$_2$X peptides goes to completion, HPLC analysis was performed on a representative set of peptide reactions. Reactions containing 3 μM dansyl-GCVa$_2$X peptide were monitored as described above until reaction completion was attained, as indicated by a plateau in the observed fluorescence. The reactions were then analyzed by HPLC (Zorbax Eclipse XDB RP-C_8 column), with a gradient from 20% acetonitrile in water containing 0.05% trifluoroacetic acid (TFA) to 100% acetonitrile containing 0.05% TFA flowing at 1 mL/min over 30 min; peptides and products were detected by fluorescence (λ_{ex} = 335 nm and λ_{em} = 486 nm). In all cases, HPLC analysis indicates that the peak for the dansyl-GCVa$_2$X peptide shifts completely to a longer retention time while exhibiting an increase in observed fluorescence, consistent with quantitative farnesylation, whereas parallel reactions performed without FTase showed no change in peptide retention time. Representative HPLC traces are included in the Supporting Information.

For most peptides, $k_{cat}/K_M^{peptide}$ was determined from a fit of the Michaelis−Menten equation to the dependence of initial velocity divided by enzyme concentration (V/E) on the peptide concentration in the presence of saturating FPP. For peptides that displayed substrate inhibition at high peptide concentrations, $k_{cat}/K_M^{peptide}$ was determined from a fit of the Michaelis−Menten equation modified to include substrate inhibition (eq 2):

$$V/E = k_{cat}\left(\frac{[peptide]}{K_M + [peptide]\left(1 + \frac{[peptide]}{K_i}\right)}\right) \quad (2)$$

Transient Kinetics. Single-turnover assays were performed in 50 mM HEPPSO buffer, pH 7.8, 5 mM TCEP, and 5 mM $MgCl_2$ in the presence of *N*-[2-(1-maleimidyl)ethyl]-7-(diethylamino)coumarin-3-carboxamide-labeled phosphate binding protein (MDCC-labeled PBP) (*38*) and inorganic pyrophosphatase (PP_iase) to measure the formation of diphosphate (*39*). Phosphate binding protein was purified and labeled with *N*-[2-(1-maleimidyl)ethyl]-7-(diethylamino)coumarin-3-carboxamide (MDCC) as in previous studies (*26, 39*). FTase was preincubated with FPP for 15 min at room temperature; the reactions were initiated by addition of dansyl-GCVa_2X peptide, MDCC-labeled PBP, and PP_iase. The final concentrations were 800 nM FTase, 200 nM FPP, 25 μM dansyl-GCVa_2X peptide, 5 μM MDCC-PBP, and 34 units mL^{-1} PP_iase. A KinTek stopped-flow instrument (KinTek Corp., Austin, TX) was used to monitor the binding of inorganic phosphate to the MDCC-labeled PBP, which is observed as an increase in fluorescence (λ_{ex} = 430 nm cutoff filter, λ_{em} = 450 nm cutoff filter). Prior to reactions, the KinTek stopped-flow instrument was treated with a "phosphate mop" consisting of 0.5 units mL^{-1} purine nucleoside phosphorylase and 15 μM 7-methylguanosine in 50 mM HEPPSO, pH 7.8, 5 mM TCEP, and 5 mM $MgCl_2$ to sequester any monophosphate contaminants (*26, 39*).

Under these conditions, the rate of cleavage of the pyrophosphate product catalyzed by PP_iase and the association rate for phosphate binding to MDCC-labeled PBP are fast relative to the rate constant for diphosphate formation and release catalyzed by the prenyltransferases (*39*). The rate constant for product formation (k_{STO}) was determined by fitting eq 3 to the fluorescence change as a function of time, where Fl_{obs} is observed fluorescence, Amp is amplitude, k_{STO} is the observed rate constant, and Fl_{init} is the initial fluorescence. The observed rate constant k_{STO} is described by eq 4, derived from a reversible two-step kinetic mechanism proceeding from the E·FPP·peptide complex as shown in Scheme 2 (*40*).

$$Fl_{obs} = Amp(1 - e^{-k_{STO}t}) + Fl_{init} \quad (3)$$

$$k_{STO} = \frac{k_{conf}k_{chem}}{k_{conf} + k_{-conf} + k_{chem}} \quad (4)$$

Calculation of Relative Peptide Reactivity. For each peptide panel (dansyl-GCVa_2A, dansyl-GCVa_2S, dansyl-GCVa_2Q, and dansyl-GCVa_2M), $-\Delta\Delta G$ was calculated relative to the reactivity of the panel peptide with glycine at the a_2 position according to eq 5, where *R* is the gas constant and *T* is the assay temperature (298 K), unless noted otherwise. For steady-state turnover, $k_{cat}/K_M^{peptide}$ values from Table 1 are used in eq 5. For single-turnover reactions, k_{STO} values from Table 2 are used in eq 5.

$$-\Delta\Delta G(k^{peptide}) = RT\ln\left(\frac{k^{dns\text{-}GCVa_2X}}{k^{dns\text{-}GCVGX}}\right) \quad (5)$$

RESULTS

FTase-Catalyzed Farnesylation of Peptides Depends on the Amino Acid at a_2. The initial peptide sequences were based on the C-terminal sequence of H-Ras (-CVLS), an extensively studied prenylated human protein. We first measured the steady-state kinetic parameters for FTase-catalyzed farnesylation of 20 peptides of the form dansyl-GCVa_2S; this panel randomizes the a_2 residue while maintaining the rest of the H-Ras Ca_1a_2X sequence constant. FTase-catalyzed farnesylation is observed for 19 of the 20 peptides (excluding GCVRS) using a fluorescence-based assay (*35, 37*) (Table 1). The values for $k_{cat}/K_M^{peptide}$ are reported in Table 1, as this is the most relevant parameter for specificity in the presence of competing substrates (*41*). Nonetheless, the value of this parameter varies by a factor of nearly 10^5-fold as the identity of the amino acid at the a_2 residue varies. The values of k_{cat} for a subset of peptides are reported in Supporting Information. Subsequent radioactive assays indicate that FTase catalyzes farnesylation of dansyl-GCVRS slowly with an apparent value for $k_{cat}/K_M < 1000$ M^{-1} s^{-1}, which is comparable to that of the other peptides containing a charged a_2 residue (i.e., $k_{cat}/K_M^{dansyl\text{-}GCVKS} = 270$ M^{-1} s^{-1}). These data indicate that the arginine residue in the a_2 position minimizes the change in dansyl fluorescence that occurs upon farnesylation (data not shown).

Table 2: Single-Turnover Rate Constants (k_{STO}) for Farnesylation of Dansyl-GCVa_2S and Dansyl-GCVa_2M Peptides Catalyzed by FTase

	k_{STO} (s^{-1})[a]	
a_2	X = S	X = M
G	0.092 ± 0.004	0.26 ± 0.01
A	1.4 ± 0.1	4.7 ± 0.1
S	0.84 ± 0.08	2.1 ± 0.2
T	3.2 ± 0.2	6.2 ± 0.4
V	6.9 ± 0.9	6.5 ± 0.3
M	6.5 ± 0.8	8.7 ± 0.6
I	3.5 ± 0.1	7.9 ± 0.3
L	3.8 ± 0.5	4.7 ± 0.2
F	0.41 ± 0.02	2.7 ± 0.1
W	0.11 ± 0.01	1.5 ± 0.1

[a] Single-turnover farnesylation rate constants were determined using a fluorescence-based assay as described in Materials and Methods.

To examine the basis for substrate selectivity at the a_2 position using structure−function analysis, we correlate relative values of $k_{cat}/K_M^{peptide}$ for various peptides with both the hydrophobicity (as indicated by $\Delta G_{transfer}$ of the side chain between octanol and water) and steric volume of the a_2 residue (*42, 43*). The relative peptide reactivity is expressed as the value of $-\Delta\Delta G(k_{cat}/K_M^{peptide})$ (eq 5 in Materials and Methods) comparing the reactivity of a peptide with an altered sequence at a_2 to the peptide with glycine at this position. A complication of this analysis is that for many amino acids hydrophobicity correlates linearly with steric volume (Figure 2a) (*42, 43*), making identification of the important parameters for selectivity more difficult. For the dansyl-GCVa_2S peptides, FTase reactivity is maximal for a_2 residues with $\Delta G_{transfer}$ of ~1.7 kcal/mol, e.g., valine and methionine (Figure 2b). For small "nonpolar" amino acids, as defined in the legend of Figure 2a, the relative peptide reactivity with FTase correlates with the hydrophobicity (as measured by $\Delta G_{transfer}$) of the a_2 residue. The reactivity of FTase with a peptide substrate (as indicated by $-\Delta\Delta G(k_{cat}/K_M^{peptide})$) trends sharply downward as hydrophobicity at the a_2 position decreases below the $\Delta G_{transfer}$ for glycine (~0 kcal/mol) (slope = 4.8 ± 0.9, R^2 = 0.89), consistent with the Ca_1a_2X box paradigm. However, reactivity also decreases for large hydrophobic amino acids such as phenylalanine and

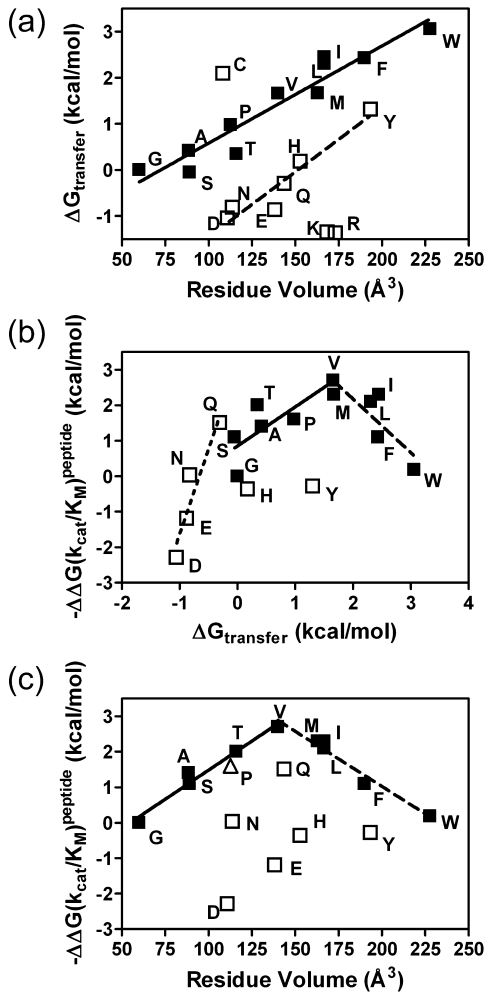

FIGURE 2: Reactivity of FTase with dansyl-GCVa_2S peptides correlates with the hydrophobicity and steric volume of the a_2 residue. (a) Correlation of $\Delta G_{transfer}$, indicative of amino acid hydrophobicity (*42*), with steric volume (*43*). For amino acids that lie on the solid black line (G, A, S, P, T, V, I, L, M, F, and W; filled squares) hereafter referred to as the "nonpolar" amino acids, hydrophobicity is proportional to steric volume (slope = 0.021 ± 0.002, $R^2 = 0.91$). A second group of more polar amino acids (D, E, N, Q, H, Y, K, R, and C; open squares) also shows a correlation between hydrophobicity and volume (slope = 0.028 ± 0.004, $R^2 = 0.91$) although they fall on a different line. Three amino acids (C, K, and R) appear to be outliers. (b) Correlation between the relative reactivity of FTase with dansyl-GCVa_2S peptides and the hydrophobicity of the a_2 residue. The solid (a_2 = G, A, S, T, P, and V; slope = 1.1 ± 0.4, $R^2 = 0.63$) and dashed (a_2 = V, M, I, L, F, and W; slope = −1.5 ± 0.5, $R^2 = 0.72$) lines are linear fits to the relative reactivities of FTase with the "nonpolar" amino acids. The dotted line (slope = 4.8 ± 0.9, $R^2 = 0.89$) is a linear fit to the reactivities of FTase with a subset of the polar amino acids (D, E, N, and Q). The $-\Delta\Delta G(k_{cat}/K_M^{peptide})$ values are calculated relative to dansyl-GCVGS as described in Materials and Methods from $k_{cat}/K_M^{peptide}$ values reported in Table 1. Symbols are identical to those described in (a). (c) Correlation between FTase reactivity with dansyl-GCVa_2S peptides and the steric volume of the a_2 residue. The solid and dotted lines are linear fits to the relative reactivities of FTase with the "nonpolar" amino acids described in (a). The solid line (encompassing "nonpolar" amino acids with volumes ≤140 Å^3) has a slope of 0.033 ± 0.003 kcal/(mol·Å^3) ($R^2 = 0.97$), and the dotted line (including "nonpolar" amino acids with volumes ≥140 Å^3) has a slope of −0.031 ± 0.003 kcal/(mol·Å^3) (R^2 = 0.96). The $-\Delta\Delta G(k_{cat}/K_M^{peptide})$ values are calculated relative to dansyl-GCVGS as described in Materials and Methods from $k_{cat}/K_M^{peptide}$ values reported in Table 1. Symbols are identical to those described in (a), except for proline being represented by an open triangle.

Scheme 1

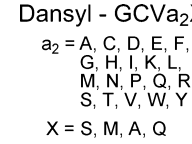

tryptophan, indicating that increased reactivity due to favorable hydrophobic contacts alone does not determine selectivity at the a_2 position.

When correlated with the steric volume of the amino acid at the a_2 position, the relative peptide reactivity with FTase displays a maximum near the steric volume of valine at 140 Å^3 (Figure 2c). In this plot, the data cluster into two groups per the two trend lines shown in Figure 2a. "Nonpolar" amino acids (solid squares) form a pyramidal pattern peaking at 140 Å^3. The polar and charged amino acids (open squares) fall below the pyramidal curve in an apparent scatter plot, indicating that the volume of the a_2 residue is not the main determinant of reactivity for amino acids with hydrophilic side chains. An increase in the polarity at a given steric volume of the amino acid at the a_2 position of the peptide leads to decreased reactivity, as also illustrated in Figure 2b. This lower reactivity for polar amino acids is consistent with the hydrophobic preference previously proposed for the a_1 and a_2 positions of the Ca_1a_2X sequence. However, the decrease in reactivity for nonpolar amino acids larger than valine suggests that substrate discrimination is also based upon the steric volume of the a_2 residue. Therefore, our data support a model wherein FTase recognizes the side chains at the a_2 position of potential substrates based upon both size and polarity.

Determining the Effect of Changing the X Residue on a_2 Selectivity. To ascertain whether recognition of the a_2 residue by both polarity and size is a general feature of FTase substrate selectivity, we measured the reactivity of FTase with peptides terminating in other X residues commonly found in naturally occurring FTase substrates: methionine, alanine, and glutamine (Scheme 1) (*16, 17, 24*). For all of these peptide panels, the reactivity of FTase with the peptides decreases with increasing polarity of the a_2 residue for the polar amino acids as defined in Figure 2a; in fact, the reactivity of FTase with some of the peptides with charged a_2 residues is below the detection limit of the fluorescence assay (Table 1). This trend indicates that the preference for hydrophobic residues at the a_2 position is general, as previously proposed (*1, 3, 14, 17, 25, 44, 45*). In contrast, for the "nonpolar" amino acids, the dependence of reactivity on the volume of the a_2 residue is dependent on the identity of the X group (Figure 3); proline-containing substrates (open triangles) are excluded from the correlation analysis as they appear to be outlier points, possibly due to changes in conformation of the peptide substrate. Peptides terminating in alanine display a reactivity trend similar to that seen with serine (Figure 3a) although the peak reactivity volume increases to ~160 Å^3. Strikingly, the reactivity of FTase with peptides ending with glutamine (Figure 3c) and methionine (Figure 3d) shows limited dependence on the volume of the a_2 residue. For these peptides, the measured reactivity plateaus and does not decrease when the residue volume is larger than ~110 Å^3. Furthermore, the increase in reactivity (as measured by $k_{cat}/K_M^{peptide}$) for the most reactive peptide

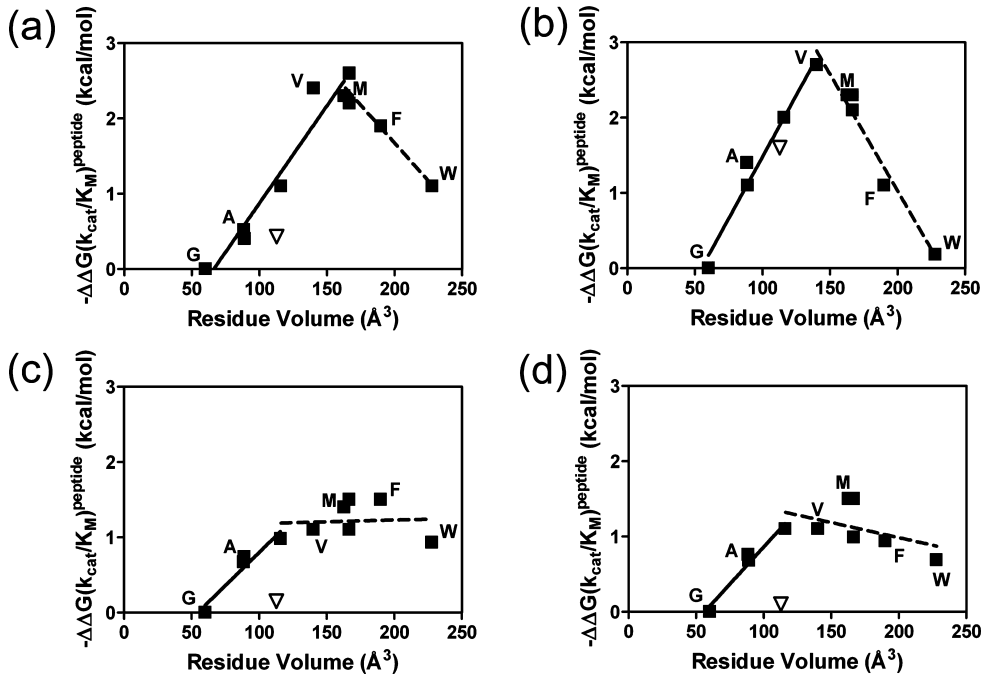

FIGURE 3: The identity of the X residue affects a_2 selectivity. For all four peptide panels, $-\Delta\Delta G(k_{cat}/K_M^{peptide})$ for ten "nonpolar" peptides is plotted versus residue volume (filled squares); proline-containing peptides are shown as an open triangle. A subset of a_2 residues (G, A, V, M, F, and W) are labeled. Linear fits were performed within the low volume (solid line) and high volume (dotted line) regions of the plot. (a) Dansyl-GCVa_2A peptide panel. The solid line has a slope of 0.026 ± 0.004 kcal/(mol·Å^3) ($R^2 = 0.93$), and the dotted line has a slope of −0.021 ± 0.003 kcal/(mol·Å^3) ($R^2 = 0.92$). (b) Dansyl-GCVa_2S peptide panel (duplicated from Figure 1c). (c) Dansyl-GCVa_2Q peptide panel. The solid line has a slope of 0.018 ± 0.004 kcal/(mol·Å^3) ($R^2 = 0.92$), and the dotted line has a zero slope within error. (d) Dansyl-GCVa_2M peptide panel. The solid line has a slope of 0.020 ± 0.003 kcal/(mol·Å^3) ($R^2 = 0.96$), and the dotted line has a zero slope within error. The $-\Delta\Delta G(k_{cat}/K_M^{peptide})$ values are calculated relative to peptides containing glycine at the a_2 position as described in Materials and Methods from $k_{cat}/K_M^{peptide}$ values reported in Table 1.

compared to the substrate with glycine at the a_2 position varies with the X group; this ratio is 91 ± 6-fold and 75 ± 6-fold with serine and alanine at the X position, respectively, compared to the smaller ratios of 14 ± 4-fold and 13 ± 2-fold with glutamine and methionine, respectively, as the X residue. This dependence of the relative reactivity of FTase with peptides containing different a_2 residues on the identity of the X residue reflects functional interconnection in recognition of these two side chains by FTase.

Comparison of the reactivity of FTase with peptides containing the same a_2 residue and different X residues reveals that alteration of the structure of the X residue results in both increases and decreases in peptide reactivity. Replacement of alanine at the X position with glutamine increases the reactivity of FTase with peptides containing either small or large nonpolar residues at the a_2 positions; in contrast, the reactivity of peptides with a_2 residues of intermediate size is unaffected (Figure 4a). When the X residue is changed from serine to glutamine (Figure 4b), the reactivity of FTase similarly increases for peptides containing small or large nonpolar a_2 residues; however, the reactivity of several peptides with a_2 residues in the middle of the volume range decreases. Similar changes in reactivity occur when the X residue is changed from serine to methionine (Supporting Information).

The Rate Constant for Peptide Farnesylation Varies with the Peptide Sequence at the a_2 Position. The rate constants for farnesylation of the "nonpolar" peptides from the dansyl-GCVa_2S and dansyl-GCVa_2M panels catalyzed by FTase were determined under single-turnover conditions using a fluorescence-based assay that detects the release of pyrophosphate following farnesylation (*38, 39*). Previous kinetic studies of FTase suggest the basic kinetic pathway shown in Scheme 2 (*34, 35, 39, 46*−*48*). Substrate binding is

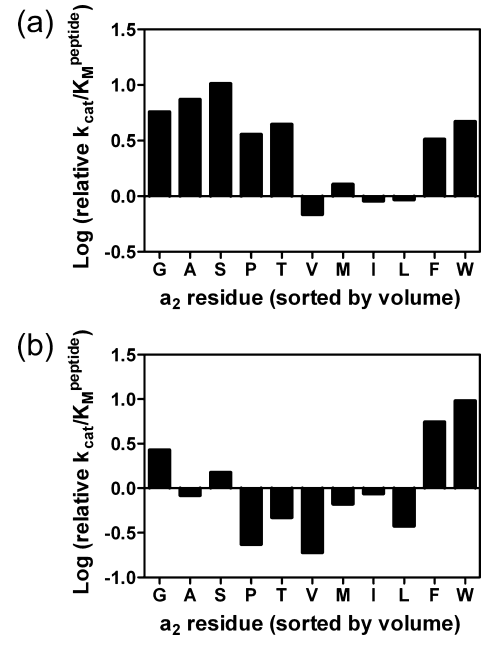

FIGURE 4: The effect of altering the X residue on reactivity of FTase with peptides. (a) Reactivities of FTase with dansyl-GCVa_2Q peptides compared to dansyl-GCVa_2A peptides. For each a_2 residue, the relative reactivity is calculated as $\log[(k_{cat}/K_M^{dansyl\text{-}GCVa_2Q})/(k_{cat}/K_M^{dansyl\text{-}GCVa_2A})]$. (b) Reactivities of FTase with dansyl-GCVa_2Q peptides compared to dansyl-GCVa_2S peptides. For each a_2 residue, the relative reactivity is calculated as $\log[(k_{cat}/K_M^{dansyl\text{-}GCVa_2Q}))/(k_{cat}/K_M^{dansyl\text{-}GCVa_2S})]$.

Scheme 2

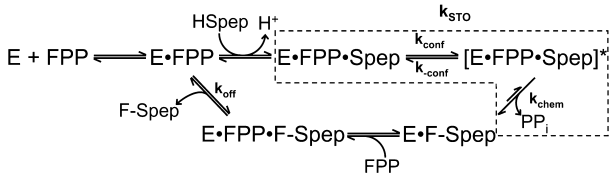

functionally ordered, with FPP binding before peptide, and the rate constant for farnesylation is faster than product dissociation under saturating (k_{cat}) multiple-turnover conditions (*46, 47, 49, 50*). The pathway also includes a conformational rearrangement of the first two isoprene units of FPP that has been proposed based on structural and mutagenesis studies (*33, 36, 51, 52*). The observed rate constant for formation of the farnesylated product, k_{STO} (dotted outline, Scheme 2), measures the formation of the E·farnesylated-peptide complex from the E·FPP·peptide ternary complex (*39, 49, 53*). This observed rate constant includes both the rate constants for the chemical step and the conformational rearrangement of FPP.

For the "nonpolar" peptides from the dansyl-GCVa$_2$S panel, values of k_{STO} vary by ~75-fold from the slowest peptide (a_2 = G) to the fastest (a_2 = V) (Table 2). The range of values for the dansyl-GCVa$_2$M "nonpolar" peptides is similar (~30-fold), but the trend of k_{STO} with a_2 residue volume is distinct from that observed with the dansyl-GCVa$_2$S peptides. When relative k_{STO} values are correlated with a_2 residue volume (Figure 5a), the peptides terminating in serine exhibit a pyramidal pattern similar, in both shape and relative energetics, to that seen for relative peptide reactivity under $k_{cat}/K_m^{peptide}$ conditions (Figure 3b). Correlation of relative k_{STO} values with a_2 residue volume for the dansyl-GCVa$_2$M peptides (Figure 5b) also strongly resembles the similar correlation with the steady-state reactivity (Figure 3d). These data demonstrate that the relative peptide reactivity of FTase under subsaturating steady-state reaction conditions mirrors the relative reactivity under single-turnover conditions.

Reactivity of Dansyl-GCVa$_2$M Peptides with W102βA and S99βA FTase Mutants. Previous structural analysis of several peptide substrates bound to FTase suggests that peptides terminating in methionine or glutamine may form hydrogen bonds with the side chains of residues W102β and S99β within the FTase active site (Figure 6); substrates with serine or alanine at the X position cannot form these interactions. To examine the functional importance of these proposed hydrogen bonds, including whether they are important for a_2 selectivity, we determined the reactivity of the W102βA and S99βA mutants with the dansyl-GCVa$_2$M peptide panel. These two alanine mutations minimally affect both the reactivity of FTase with peptides relative to WT FTase (Supporting Information) and the trend of a_2 selectivity (Figure 7). These data indicate that any contacts formed between the terminal methionine residue of the substrate and the side chains of the active site residues W102β and S99β contribute neither to acceleration of peptide substrate turnover under subsaturating conditions nor to selectivity at the a_2 position. While these contacts may be important for other steps along the FTase reaction pathway, the interactions that lead to recognition of the a_2 residue and the cross-talk between the a_2 and X residues remain functionally unaffected by these mutations.

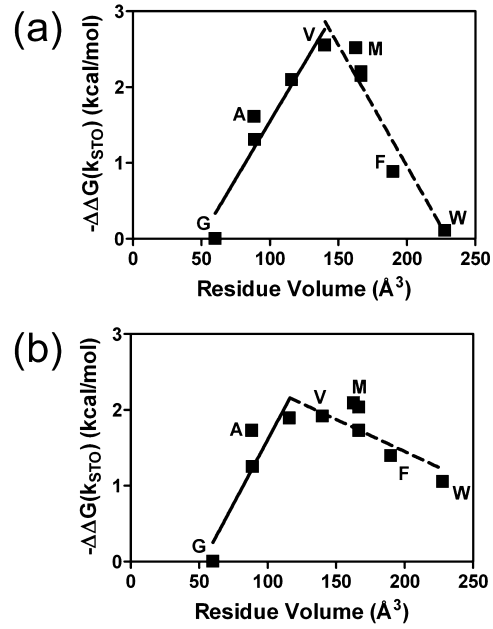

FIGURE 5: Correlation of the single turnover rate constant for farnesylation catalyzed by FTase with the volume of the a_2 residue for dansyl-GCVa$_2$S and dansyl-GCVa$_2$M peptides. For both peptide panels, $-\Delta\Delta G(k_{STO})$ for ten "nonpolar" peptides is plotted versus the a_2 residue volume (filled squares). A subset of a_2 residues (G, A, V, M, F, and W) are labeled. (a) Dansyl-GCVa$_2$S peptide panel. The solid line has a slope of 0.030 ± 0.006 kcal/(mol·Å^3) (R^2 = 0.91), and the dotted line has a slope of −0.032 ± 0.005 kcal/(mol·Å^3) (R^2 = 0.91). (b) Dansyl-GCVa$_2$M peptide panel. The solid line has a slope of 0.03 ± 0.01 kcal/(mol·Å^3) (R^2 = 0.82), and the dotted line has a slope of −0.008 ± 0.003 kcal/(mol·Å^3) (R^2 = 0.63). The $-\Delta\Delta G(k_{STO})$ values are calculated relative to peptides containing glycine at the a_2 position, as described in Materials and Methods, using the k_{STO} values reported in Table 2.

DISCUSSION

Reaction Steps Involved in Peptide Selectivity of FTase. The steady-state kinetic parameter that best reflects the selectivity of an enzyme for different substrates is k_{cat}/K_M (*41*). In FTase, the steady-state parameter $k_{cat}/K_M^{peptide}$ includes the rate constants for reaction steps from peptide binding to the E·FPP complex through farnesylation and dissociation of diphosphate, which is the first irreversible step (*47, 51, 52*). In contrast, peptide farnesylation catalyzed by FTase measured under single-turnover conditions (with saturating enzyme) monitors only steps that occur after peptide binding and prior to diphosphate release (Scheme 2) (*26, 39*). Therefore, single-turnover kinetics in the presence of limiting FPP (relative to [E]) isolates the farnesylation step from the product release steps and includes the FPP conformational change and farnesylation of the peptide (*49, 53*). The similarity of the dependence of the values of $k_{cat}/K_M^{peptide}$ and k_{STO} for FTase on the peptide sequence suggests that the same reaction step(s) are rate-limiting under both conditions and indicates that the observed peptide specificity is not significantly dependent on peptide binding. Based on this correlation, FTase-catalyzed farnesylation of peptide substrates under $k_{cat}/K_M^{peptide}$ conditions appears to be limited by the rate constants for either or both the conformational rearrangement of FPP and/or the chemical step. As multiple studies have

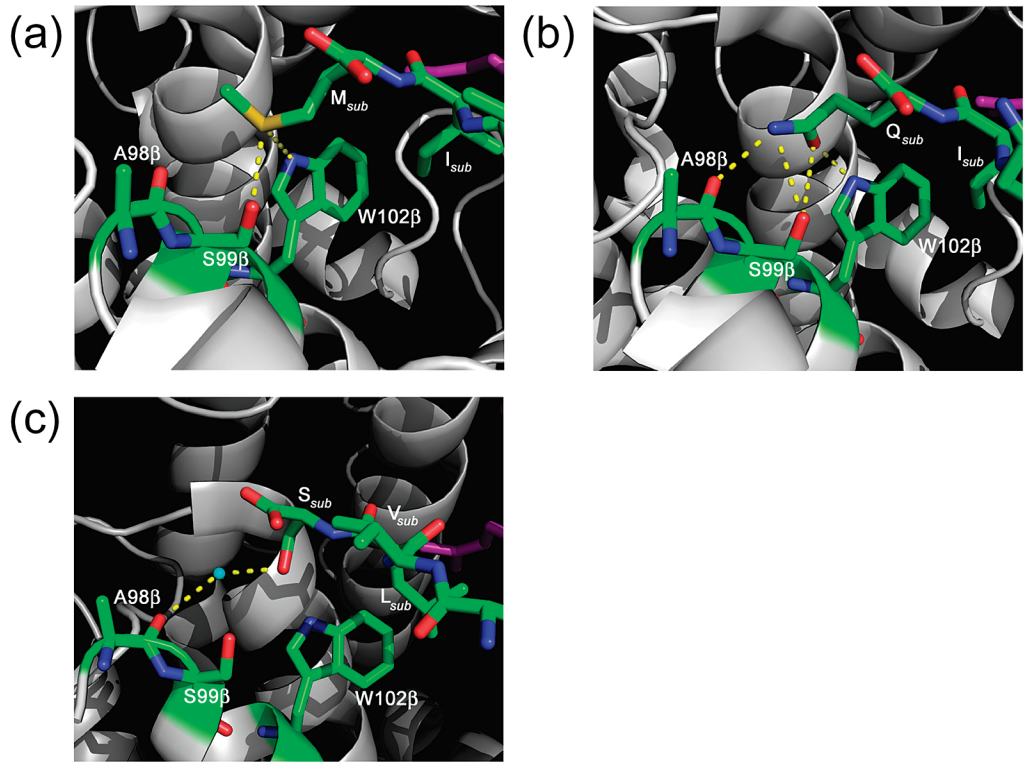

FIGURE 6: Crystallographic contacts observed between the X residue of the Ca_1a_2X sequence and the FTase active site. Proposed hydrogen bond contacts are shown as dashed lines between heteroatoms, and distances were measured between heteroatoms involved in the proposed hydrogen bond. In each case, the peptide substrates are complexed with FTase and the FPP analogue inhibitor FPT-II. Peptide substrate residues are denoted with a "sub" subscript. Figures are adapted from ref *10*. (a) Complex of a KKKSKTKCVIM substrate with FTase and FPT-II (PDB ID 1D8D). The substrate methionine sulfur is positioned to form hydrogen bonds with the side chain hydroxyl of S99β (3.2 Å) and side chain indole nitrogen of W102β (3.5 Å). (b) Complex of a DDPTASACNIQ substrate with FTase and FPT-II (PDB ID 1TN6). The amide oxygen of the glutamine side chain in the peptide substrate is proposed to hydrogen bond with the side chain indole nitrogen of W102β (2.8 Å) and side chain hydroxyl of S99β (3.5 Å), and the amide nitrogen is near the side chain hydroxyl of S99β (3.4 Å) and the backbone carbonyl oxygen of A98β (2.9 Å). (c) Complex of a GCVLS substrate with FTase and FPT-II (PDB ID 1TN8). The substrate serine hydroxyl group is positioned to form a hydrogen bond with the backbone carbonyl oxygen of A98β through a water molecule (blue sphere), with distances of 2.7 Å from the serine hydroxyl group oxygen to the water molecule oxygen and 3.0 Å from the water to the backbone carbonyl oxygen of A98β.

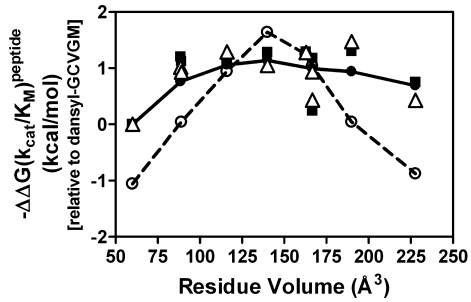

FIGURE 7: Substitution of the S99β and W102β side chains with alanine does not alter a_2 selectivity in the dansyl-GCVa_2M peptide panel. Relative reactivities for dansyl-GCVa_2M peptides with W102βA (filled squares) and S99βA (open triangles) mutant FTases are plotted versus the steric volume of the a_2 residue; $-\Delta\Delta G(k_{cat}/K_M^{peptide})$ values are calculated relative to dansyl-GCVGM as described in Materials and Methods from $k_{cat}/K_M^{peptide}$ values reported in Table 2. $-\Delta\Delta G(k_{cat}/K_M^{peptide})$ values for reaction of dansyl-GCVa_2M peptides (solid line with filled circles) and dansyl-GCVa_2S peptides (dotted line with open circles) with WT FTase are plotted for comparison; $-\Delta\Delta G(k_{cat}/K_M^{peptide})$ values for peptide reactivity with WT FTase are all calculated relative to reactivity with dansyl-GCVGM.

shown that product release is rate-limiting under k_{cat} conditions (*39, 48*), these data indicate that different reaction steps are rate-limiting for FTase under subsaturating ($k_{cat}/K_M^{peptide}$) and saturating (k_{cat}) steady-state conditions. Consistent with this conclusion, the value of k_{cat} has a significantly altered dependence on substrate structure (see Supporting Information) compared to $k_{cat}/K_M^{peptide}$. In summary, peptide selectivity under $k_{cat}/K_M^{peptide}$ conditions reflects sequence-dependent modulation of the chemical step and/or the conformational rearrangement of FPP prior to farnesylation.

Interactions Potentially Involved in a_2 Recognition. Depending on the peptide sequence context, selectivity at the a_2 position presumably involves both positive hydrophobic and negative steric interactions. This dual selectivity is consistent with predictions from both structural and bioinformatic studies (*9, 10*); structural data yield insight into which groups may interact with the a_2 side chain to transduce recognition (*10*). The a_2 binding site in FTase is formed by residues W102β, W106β, and Y361β, as well as the third isoprenoid unit of the FPP co-substrate (Figure 1). This hydrophobic, tightly packed binding site appears well designed to bind moderately sized nonpolar amino acids. Mutations of these residues have been shown to affect enzyme behavior, in one case transforming FTase into a GGTase (*54, 55*), indicating that these residues play important roles within the FTase active site. Studies combining mutagenesis at these positions with structure−function analysis of peptide reactivity provide valuable insight into the identity, nature, and energetic contributions of interactions used by FTase for substrate recognition.

Dependence of a_2 Selectivity on the X Residue. The reactivity of FTase with peptides depends on identity of both the a_2 and X residues (Tables 1 and 2), consistent with previous measurements of FTase selectivity (*1, 14, 17, 24*−*27, 45, 56*); furthermore, the identity of the X residue affects the FTase selectivity at the a_2 position under both steady-state and single-turnover conditions. This type of cross-talk in recognition of peptide substrates has previously been observed with other enzymes, including proteinases. Context-dependent recognition of side chains in peptide substrates has been extensively evaluated for several well-studied serine proteases, such as trypsin and chymotrypsin, leading to models wherein substrate−enzyme interactions far from the cleavage site can dramatically affect catalysis through substrate alignment, inducing favorable conformational changes, and other potential mechanisms (reviewed in ref *57*).

We envision two types of potential mechanisms that could lead to the observed dependence of the a_2 selectivity on the X group in FTase: one mechanism is a change in rate-limiting steps where the two potential rate-limiting steps have a differential dependence on the peptide sequence, and a second mechanism is alteration of the structure of the FTase·peptide complex (discussed further below). As described above, the rate-limiting step under single turnover and multiple turnover with subsaturating peptide conditions could be either the FPP conformational change required to form an active FTase·FPP·peptide ternary complex or farnesylation of the peptide from this active complex. Kinetic isotope effect experiments performed under single-turnover conditions have demonstrated that the rate-limiting step alters with the structure of the peptide substrate, varying from rate-limiting conformational rearrangement of FPP for the peptide GCVLS to rate-limiting farnesylation for the peptide TGCVIM (*40, 58*). Therefore, the a_2−X cross-talk in the peptide specificity data could be caused by these two kinetic steps having a differential dependence on the side chain structure of the amino acids at the X and the a_2 positions leading to changes in the rate-limiting step as the peptide sequence varies. The isotope effect and single-turnover data suggest that the X-group mainly affects the rate constants for the conformational rearrangement (Table 2, *26, 40, 58*). By analogy, we propose that the conformational rearrangement is the main rate-contributing step in farnesylation of dansyl-GCVGS catalyzed by FTase. If alteration of the X group to methionine (dansyl-GCVGM) changes the main rate-contributing step to farnesylation by enhancing the conformation rate constant, as previously observed for TGCVIM, then the dependence of the observed rate constants on the structure of the a_2 position will also change. While the extensive structural contacts observed between the peptide substrate and the isoprenoid tail of FPP may suggest that modulation of the conformational rearrangement step serves as the primary mechanism for modulating peptide reactivity (*10, 36, 59*), further kinetic isotope effect experiments will be required to deconvolute the sequence-dependent interplay of the chemical and conformational rearrangement steps potentially responsible for FTase peptide selectivity.

Structural Insights into the Mechanism of a_2−X Cross-Talk. As stated above, an alternative mechanism for the observed dependence of the a_2 selectivity on the X group involves alternate binding modes for the peptide substrate. Peptides terminating in glutamine or methionine could form contacts within the FTase·peptide complex that are absent when the X residue is serine or alanine, with these interactions leading to changes in a_2 specificity. The functional interactions that would transduce the observed a_2−X residue cross-talk are presumably located within the FTase active site near to the peptide substrate. Crystal structures of peptide substrates KKKSKTKCVIM (PDB 1D8D) (*59*), DDPTASACNIQ (PDB 1TN6) (*10*), and GCVLS (PDB 1TN8) (*10*) allow comparison of the observed contacts made by the various X residues with side chains within the FTase active site, specifically within the FTase β subunit (Figure 6). While the peptide and FPP analogue bound to FTase in these complexes are not positioned in a conformation that can readily react (*10, 52, 59*), the conformational changes required to form an active ternary complex are not proposed to require repositioning of the a_2 or X residues of the peptide substrate (*51, 52*). In these FTase·peptide complexes, both methionine and glutamine at the X position appear to be within reasonable hydrogen-bonding distance of the imine hydrogen of W102β as well as the side chain hydroxyl group of S99β. Furthermore, in the crystal structure glutamine appears to also form a hydrogen bond with the main chain carbonyl group of A98β. In contrast, the serine in the GCVLS substrate appears to only form a water-mediated hydrogen bond to the backbone carbonyl of A98β (Figure 6c). The structurally observed contacts between methionine or glutamine at the X position and S99β and W102β may be responsible for the relative loss of a_2 residue selectivity. However, removal of the side chains of S99β and W102β does not significantly affect either the reactivity of FTase with peptides or the a_2 selectivity (Figure 7 and Supporting Information). These findings suggest that these structurally observed active site contacts with the X residue do not provide an energetic stabilization of the rate-limiting step(s) during multiple-turnover prenylation of target proteins at subsaturating conditions. In future studies, further mutagenesis studies within the FTase active site coupled with both steady-state and transient kinetic analysis will be used to illuminate the functional connections between the a_2 and X residues that contribute to FTase peptide specificity.

Potential for Novel FTase Substrate Sequences. This functional demonstration of context-dependent peptide substrate specificity suggests that the current Ca_1a_2X box model for FTase selectivity may actually reflect a subset of the potential FTase substrates. Given the observed functional cross-talk between the a_2 and X residues demonstrated in this work, it seems possible that some combinations of amino acids that have been predicted to be nonreactive based on the previous Ca_1a_2X box model may instead be efficient substrates for FTase due to cooperative recognition of three residues within the a_1a_2X tripeptide. Stated simply, the correct combination of "bad" a_2 and X residues may lead to a "good" substrate. For example, for proteins with a -Ca_1a_2X box ending in methionine or glutamine, the a_2 residue could be a variety of amino acids (i.e., I, L, V, T, M, F, W, Y, and Q) rather than the predicted hydrophobic amino acids (i.e., I, L, V, and T). As a result, human proteins such as GPI inositol-deacylase (-CNFM), brorin (-CRQM), beta-defensin 111 (-CLQQ), coiled-coil domain-containing protein 99 (-CPQQ), Rab-37 (-CSFM), and cystatin-M (-CVQM) may be efficient substrates for farnesylation catalyzed by FTase;

measurement of the reactivity of peptides containing the Ca_1a_2X sequences from Rab-37 and cystatin-M suggests that these proteins may be farnesylated (K. Hicks, H. Hartman, R. Kelly, J. L. Hougland, and C. A. Fierke, unpublished experiments). If this phenomenon of context-dependent substrate recognition extends to the a_1 residue as well, the potential for noncanonical FTase substrates would be commensurately increased. A scan of the ExPASy Swiss-Prot database for open reading frames within the human genome containing a cysteine as the fourth amino acid from the projected ORF C-terminus returns 591 proteins (*60*), with many of these terminating in sequences that do not rigorously obey the canonical Ca_1a_2X sequence. Context-dependent protein substrate recognition by FTase could substantially increase the potential number of FTase substrates within this pool of human proteins. Further characterization of the substrate recognition mechanism employed by FTase is needed to allow for accurate prediction of the full complement of prenylation substrates within the human proteome.

Context-dependent a_2 selectivity suggests that FTase recognizes the sequence downstream of the conserved cysteine as a set of two or three cooperative, interconnected recognition elements. These findings raise the possibility that protein substrates whose C-terminal sequences do not conform to the canonical Ca_1a_2X motif may be farnesylated by FTase. By providing a better understanding of the features necessary for substrate recognition and catalysis by FTase, this work will aid in both designing new FTase inhibitors as anticancer and antiparasitic agents and characterizing proteins involved in prenylation-dependent cellular signaling and regulatory pathways. Furthermore, the functional mechanism by which a_2 and X residue recognition is transduced to changes in peptide reactivity presents an appealing system for studying the interplay of molecular recognition and catalysis in a biological context.

ACKNOWLEDGMENT

We thank Elaina Zverina, Teng Xue, Soumen Chakraborty, and Animesh Aditya for help with data collection and analysis. We also thank members of the Fierke group for helpful comments and suggestions on the manuscript.

SUPPORTING INFORMATION AVAILABLE

Values of $k_{cat}/K_M^{peptide}$ for WT, W102βA, and S99βA FTases catalyzing farnesylation of dansyl-GCVa_2M peptides; values of k_{cat} for WT FTase catalyzing farnesylation of dansyl-GCVa_2X peptides; representative data illustrating analysis of FTase-catalyzed farnesylation of dansylated peptides; the effect of altering the X residue from alanine or serine to methionine on peptide reactivity; HPLC chromatograms of analysis of dansyl-GCVa_2X peptide farnesylation. This material is available free of charge via the Internet at http://pubs.acs.org.

REFERENCES

1. Zhang, F. L., and Casey, P. J. (1996) Protein prenylation: Molecular mechanisms and functional consequences. *Annu. Rev. Biochem. 65*, 241–269.
2. Benetka, W., Koranda, M., and Eisenhaber, F. (2006) Protein prenylation: An (almost) comprehensive overview on discovery history, enzymology, and significance in physiology and disease. *Monatsh. Chem. 137*, 1241–1281.
3. Casey, P. J., and Seabra, M. C. (1996) Protein prenyltransferases. *J. Biol. Chem. 271*, 5289–5292.
4. Casey, P. J. (1994) Lipid modifications of G proteins. *Curr. Opin. Cell Biol. 6*, 219–225.
5. Marshall, C. J. (1993) Protein prenylation: A mediator of protein-protein interactions. *Science 259*, 219–225.
6. Sebti, S. M., and Hamilton, A. D. (2001) *Farnesyltransferase inhibitors in cancer therapy*, Vol. 8, Humana Press, Totowa, NJ.
7. Kho, Y., Kim, S. C., Jiang, C., Barma, D., Kwon, S. W., Cheng, J. K., Jaunbergs, J., Weinbaum, C., Tamanoi, F., Falck, J., and Zhao, Y. M. (2004) A tagging-via-substrate technology for detection and proteomics of farnesylated proteins. *Proc. Natl. Acad. Sci. U.S.A. 101*, 12479–12484.
8. Maurer-Stroh, S., Koranda, M., Benetka, W., Schneider, G., Sirota, F., and Eisenhaber, F. (2007) Towards complete sets of farnesylated and geranylgeranylated proteins. *PLoS Comput. Biol. 3*, e66.
9. Maurer-Stroh, S., and Eisenhaber, F. (2005) Refinement and prediction of protein prenylation motifs. *Genome Biol. 6*, R55.
10. Reid, T. S., Terry, K. L., Casey, P. J., and Beese, L. S. (2004) Crystallographic analysis of caax prenyltransferases complexed with substrates defines rules of protein substrate selectivity. *J. Mol. Biol. 343*, 417–433.
11. Chen, Z., Sun, J. Z., Pradines, A., Favre, G., Adnane, J., and Sebti, S. M. (2000) Both farnesylated and geranylgeranylated rhob inhibit malignant transformation and suppress human tumor growth in nude mice. *J. Biol. Chem. 275*, 17974–17978.
12. Maurer-Stroh, S., Washietl, S., and Eisenhaber, F. (2003) Protein prenyltransferases: Anchor size, pseudogenes and parasites. *Biol. Chem. 384*, 977–989.
13. Gelb, M. H., Van Voorhis, W. C., Buckner, F. S., Yokoyama, K., Eastman, R., Carpenter, E. P., Panethymitaki, C., Brown, K. A., and Smith, D. F. (2003) Protein farnesyl and N-myristoyl transferases: Piggy-back medicinal chemistry targets for the development of antitrypanosomatid and antimalarial therapeutics. *Mol. Biochem. Parasitol. 126*, 155–163.
14. Caplin, B. E., Hettich, L. A., and Marshall, M. S. (1994) Substrate characterization of the saccharomyces cerevisiae protein farnesyltransferase and type-I protein geranylgeranyltransferase. *Biochim. Biophys. Acta 1205*, 39–48.
15. Omer, C. A., Karl, A. M., Diehl, R. E., Prendergast, G. C., Powers, S., Allen, C. M., and Kohl., N. E. (1993) Characterization of recombinant human farnesyl-protein transferase: Cloning, expression, farnesyl diphosphate binding, and functional homology with yeast prenyl-protein transferases. *Biochemistry 32*, 5167–5176.
16. Reiss, Y., Seabra, M. C., Armstrong, S. A., Slaughter, C. A., and Brown., M. S. (1991) Nonidentical subunits of p21h-ras farnesyltransferase. Peptide binding and farnesyl pyrophosphate carrier functions. *J. Biol. Chem. 266*, 10672–10677.
17. Moores, S. L., Schaber, M. D., Mosser, S. D., Rands, E., O'Hara, M. B., Garsky, V. M., Marshall, M. S., Pompliano, D. L., and Gibbs, J. B. (1991) Sequence dependence of protein isoprenylation. *J. Biol. Chem. 266*, 14603–14610.
18. Yokoyama, K., Goodwin, G. W., Ghomashchi, F., and Gelb., M. H. (1991) A protein geranylgeranyltransferase from bovine brain: Implications for protein prenylation specficity. *Proc. Natl. Acad. Sci. U.S.A. 88*, 5302–5306.
19. Casey, P. J., Thissen, J. A., and Moomaw., J. F. (1991) Enzymatic modification of proteins with a geranylgeranyl isoprenoid. *Proc. Natl. Acad. Sci. U.S.A. 88*, 8631–8635.
20. Fu, H. W., and Casey, P. J. (1999) Enzymology and biology of caax protein prenylation. *Recent Prog. Horm. Res. 54*, 315–342.
21. Hicks, K. A., Hartman, H. L., and Fierke, C. A. (2005) Upstream polybasic region in peptides enhances dual specificity for prenylation by both farnesyltransferase and geranylgeranyltransferase type I. *Biochemistry 44*, 15325–15333.
22. Yokoyama, K., and Gelb, M. H. (1993) Purification of a mammalian protein geranylgeranyltransferase—Formation and catalytic properties of an enzyme-geranylgeranyl pyrophosphate complex. *J. Biol. Chem. 268*, 4055–4060.
23. Yokoyama, K., McGeady, P., and Gelb, M. H. (1995) Mammalian protein geranylgeranyltransferase-I: Substrate specificity, kinetic mechanism, metal requirements, and affinity labeling. *Biochemistry 34*, 1344–1354.
24. Roskoski, R., Jr., and Ritchie, P. (1998) Role of the carboxyterminal residue in peptide binding to protein farnesyltransferase and protein geranylgeranyltransferase. *Arch. Biochem. Biophys. 356*, 167–176.
25. Reiss, Y., Stradley, S. J., Gierasch, L. M., Brown, M. S., and Goldstein, J. L. (1991) Sequence requirement for peptide recogni-

tion by rat brain p2l ras protein farnesyltransferase. *Proc. Natl. Acad. Sci. U.S.A. 88*, 732–736.
26. Hartman, H. L., Hicks, K. A., and Fierke, C. A. (2005) Peptide specificity of protein prenyltransferases is determined mainly by reactivity rather than binding affinity. *Biochemistry 44*, 15314–15324.
27. Reigard, S. A., Zahn, T. J., Haworth, K. B., Hicks, K. A., Fierke, C. A., and Gibbs, R. A. (2005) Interplay of isoprenoid and peptide substrate specificity in protein farnesyltransferase. *Biochemistry 44*, 11214–11223.
28. Krzysiak, A. J., Rawat, D. S., Scott, S. A., Pais, J. E., Handley, M., Harrison, M. L., Fierke, C. A., and Gibbs, R. A. (2007) Combinatorial modulation of protein prenylation. *ACS Chem. Biol. 2*, 385–389.
29. Troutman, J. M., Subramanian, T., Andres, D. A., and Spielmann, H. P. (2007) Selective modification of caax peptides with ortho-substituted anilinogeranyl lipids by protein farnesyl transferase: Competitive substrates and potent inhibitors from a library of farnesyl diphosphate analogues. *Biochemistry 46*, 11310–11321.
30. Hightower, K. E., Casey, P. J., and Fierke, C. A. (2001) Farnesylation of nonpeptidic thiol compounds by protein farnesyltransferase. *Biochemistry 40*, 1002–1010.
31. Goldstein, J. L., Brown, M. S., Stradley, S. J., Reiss, Y., and Gierasch, L. M. (1991) Nonfarnesylated tetrapeptide inhibitors of protein farnesyltransferase. *J. Biol. Chem. 266*, 15575–15578.
32. Riddles, P. W., Blakeley, R. L., and Zerner., B. (1979) Ellman's reagent: 5,5′-dithiobis(2-nitrobenzoic acid)—A reexamination. *Anal. Biochem. 94*, 75–81.
33. Bowers, K. E., and Fierke, C. A. (2004) Positively charged side chains in protein farnesyltransferase enhance catalysis by stabilizing the formation of the diphosphate leaving group. *Biochemistry 43*, 5256–5265.
34. Zimmerman, K. K., Scholten, J. D., Huang, C. C., Fierke, C. A., and Hupe, D. J. (1998) High-level expression of rat farnesyl:protein transferase in *Escherichia coli* as a translationally coupled heterodimer. *Protein Expression Purif. 14*, 395–402.
35. Pompliano, D. L., Gomez, R. P., and Anthony, N. J. (1992) Intramolecular fluorescence enhancement: A continuous assay of ras farnesyl:protein transferase. *J. Am. Chem. Soc. 114*, 7945–7946.
36. Long, S. B., Hancock, P. J., Kral, A. M., Hellinga, H. W., and Beese, L. S. (2001) The crystal structure of human protein farnesyltransferase reveals the basis for inhibition by CAAX tetrapeptides and their mimetics. *Proc. Natl. Acad. Sci. U.S.A. 98*, 12948–12953.
37. Cassidy, P. B., Dolence, J. M., and Poulter, C. D. (1995) Continuous fluorescence assay for protein prenyltransferases. *Methods Enzymol. 250*, 30–43.
38. Hirshberg, M., Henrik, K., Haire, L. L., Vasisht, N., Brune, M., and Webb, M. R. (1998) Crystal structure of phosphate binding protein labeled with a coumarin fluorophore, a probe for inorganic phosphate. *Biochemistry 37*, 10381–10385.
39. Pais, J. E., Bowers, K. E., Stoddard, A. K., and Fierke, C. A. (2005) A continuous fluorescent assay for protein prenyltransferases measuring diphosphate release. *Anal. Biochem. 345*, 302–311.
40. Pais, J. E. (2007) Doctoral Thesis, University of Michigan.
41. Fersht, A. (1999) *Structure and mechanism in protein science*, W. H. Freeman, New York.
42. Karplus, P. A. (1997) Hydrophobicity regained. *Protein Sci. 6*, 1302–1307.
43. Zamyatin, A. A. (1972) Protein volume in solution. *Prog. Biophys. Mol. Biol. 24*, 107–123.
44. Lowry, D. R., and Willumsen, B. M. (1989) New clue to ras lipid glue. *Nature 341*, 384–385.
45. Krzysiak, A. J., Scott, S. A., Hicks, K. A., Fierke, C. A., and Gibbs, R. A. (2007) Evaluation of protein farnesyltransferase substrate specificity using synthetic peptide libraries. *Bioorg. Med. Chem. Lett. 17*, 5548–5551.
46. Pompliano, D. L., Schaber, M. D., Mosser, S. D., Omer, C. A., Shafer, J. A., and Gibbs, J. B. (1993) Isoprenoid diphosphate utilization by recombinant human farnesyl-protein transferase—Interactive binding between substrates and a preferred kinetic pathway. *Biochemistry 32*, 8341–8347.
47. Furfine, E. S., Leban, J. J., Landavazo, A., Moomaw, J. F., and Casey, P. J. (1995) Protein farnesyltransferase: Kinetics of farnesyl pyrophosphate binding and product release. *Biochemistry 34*, 6857–6862.
48. Tschantz, W. R., Furfine, E. S., and Casey, P. J. (1997) Substrate binding is required for release of product from mammalian protein farnesyltransferase. *J. Biol. Chem. 272*, 9989–9993.
49. Huang, C. C., Hightower, K. E., and Fierke, C. A. (2000) Mechanistic studies of rat protein farnesyltransferase indicate an associative transition state. *Biochemistry 39*, 2593–2602.
50. Zhang, F. L., and Casey, P. J. (1996) Influence of metal ions on substrate binding and catalytic activity of mammalian protein geranylgeranyltransferase type-I. *Biochem. J. 320*, 925–932.
51. Long, S. B., Casey, P. J., and Beese, L. S. (2002) Reaction path of protein farnesyltransferase at atomic resolution. *Nature 419*, 645–650.
52. Pickett, J. S., Bowers, K. E., Hartman, H. L., Fu, H. W., Embry, A. C., Casey, P. J., and Fierke, C. A. (2003) Kinetic studies of protein farnesyltransferase mutants establish active substrate conformation. *Biochemistry 42*, 9741–9748.
53. Mathis, J. R., and Poulter, C. D. (1997) Yeast protein farnesyltransferase: A pre-steady-state kinetic analysis. *Biochemistry 36*, 6367–6376.
54. Spence, R. A., Hightower, K. E., Terry, K. L., Beese, L. S., Fierke, C. A., and Casey, P. J. (2000) Conversion of Tyr361 beta to Leu in mammalian protein farnesyltransferase impairs product release but not substrate recognition. *Biochemistry 39*, 13651–13659.
55. Terry, K. L., Casey, P. J., and Beese, L. S. (2006) Conversion of protein farnesyltransferase to a geranylgeranyltransferase. *Biochemistry 45*, 9746–9755.
56. Boutin, J. A., Marande, W., Petit, L., Loynel, A., Desmet, C., Canet, E., and Fauchere, J. L. (1999) Investigation of S-farnesyl transferase substrate specificity with combinatorial tetrapeptide libraries. *Cell. Signal. 11*, 59–69.
57. Hedstrom, L. (2002) Serine protease mechanism and specificity. *Chem. Rev. 102*, 4501–4524.
58. Pais, J. E., Bowers, K. E., and Fierke, C. A. (2006) Measurement of the alpha-secondary kinetic isotope effect for the reaction catalyzed by mammalian protein farnesyltransferase. *J. Am. Chem. Soc. 128*, 15086–15087.
59. Long, S. B., Casey, P. J., and Beese, L. S. (2000) The basis for k-ras4b binding specificity to protein farnesyltransferase revealed by 2 Å resolution ternary complex structures. *Structure 8*, 209–222.
60. Gasteiger, E., Gattiker, A., Hoogland, C., Ivanyi, I., Appel, R. D., and Bairoch, A. (2003) Expasy: The proteomics server for in-depth protein knowledge and analysis. *Nucleic Acids Res. 31*, 3784–3788.

BI801710G